CIS PROLINE-MEDIATED pSER5-DEPHOSPHORYLATION BY THE RNA POLYMERASE II CTD PHOSPHATASE SSU72

Jon W. Werner-Allen, Chuljin Lee, Pengda Liu, Nathan I. Nicely, Su Wang, Arno L. Greenleaf, Pei Zhou

Supplemental Material

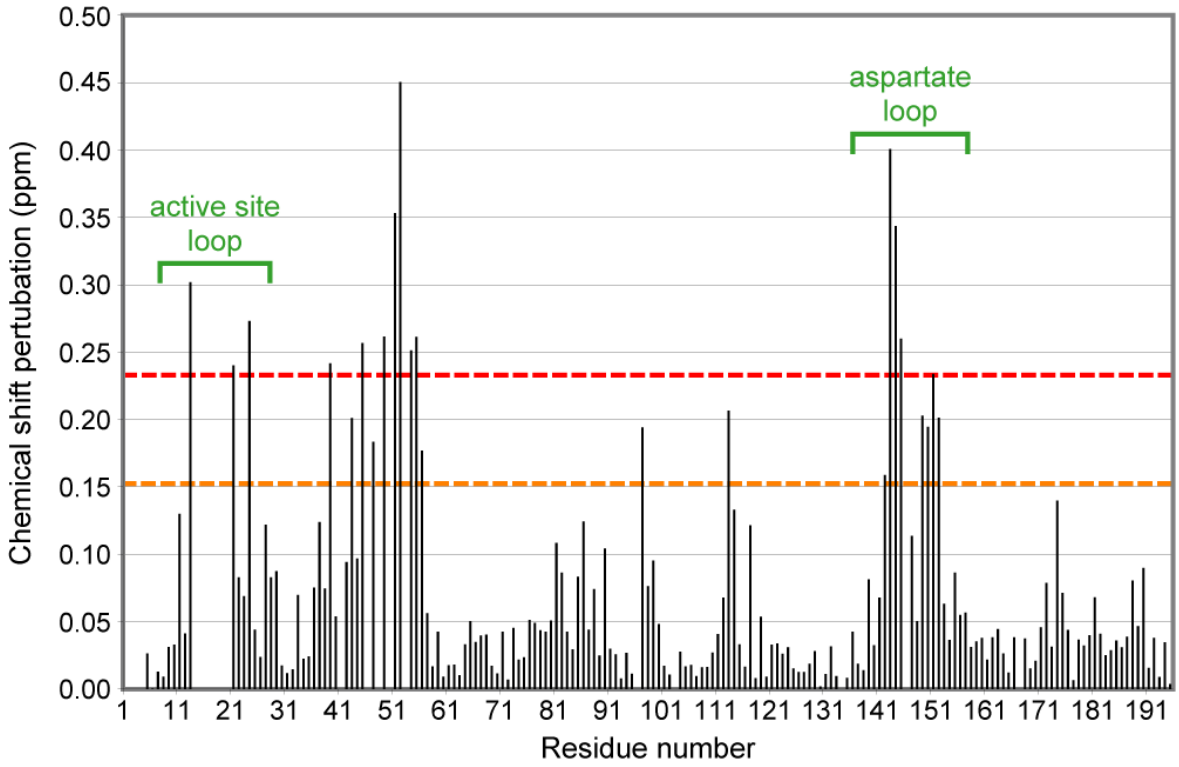

FIGURE S1. **pCTD-induced amide chemical shift perturbations for C13D/D144N dSsu72.** An interaction in the slow exchange regime on the NMR timescale was observed for the double mutant in ^{15}N-HSQC spectra. The titration endpoint was a 5:1 molar ratio of pS5 CTD peptide to enzyme. Residues without an amide peak are set to zero. Amide peaks for the phosphate-binding residues in the catalytic loop region (S14-E22) are missing, possibly due to conformational disorder in the absence of substrate (1). Orange and red dashed lines denote the 1σ and 2σ cutoff levels, respectively. Two sites of significant perturbations centered on the active site loop and aspartate loop are labeled.

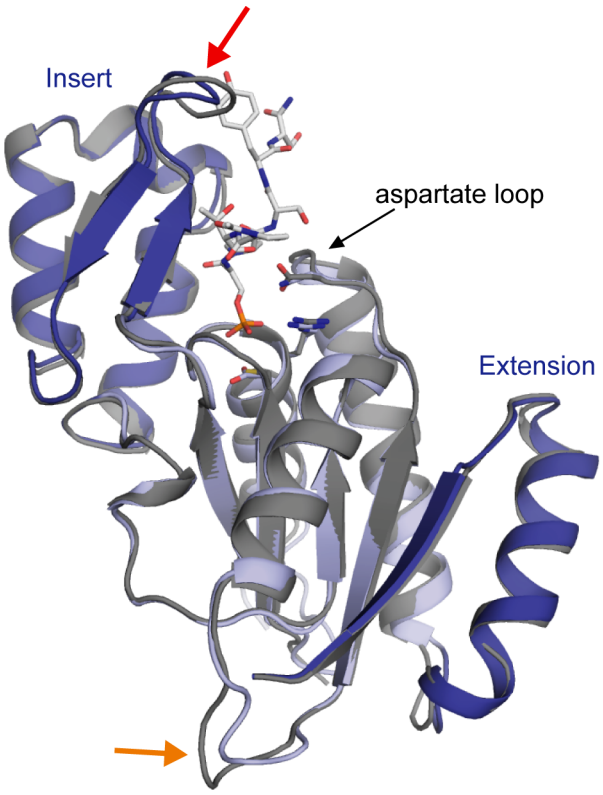

FIGURE S2. **Overlay of Ssu72 in the apo (gray) and substrate-bound (blue) form.** Substrate peptide and important catalytic residues are shown as sticks. The substrate-bound structure is colored to match Figure 1B in the main text. While pCTD binding does not induce any large-scale conformational changes ($RMSD_{backbone}$ = 0.53 Å), there are two local structural differences: (1) in the loop between the β-strands of the insert subdomain (red arrow), which contacts the aromatic ring of residue Y1 in the pCTD peptide; and (2) in the loop preceding the final β-strand of the core fold (orange arrow), which may result from distinct crystal contacts in the two structures.

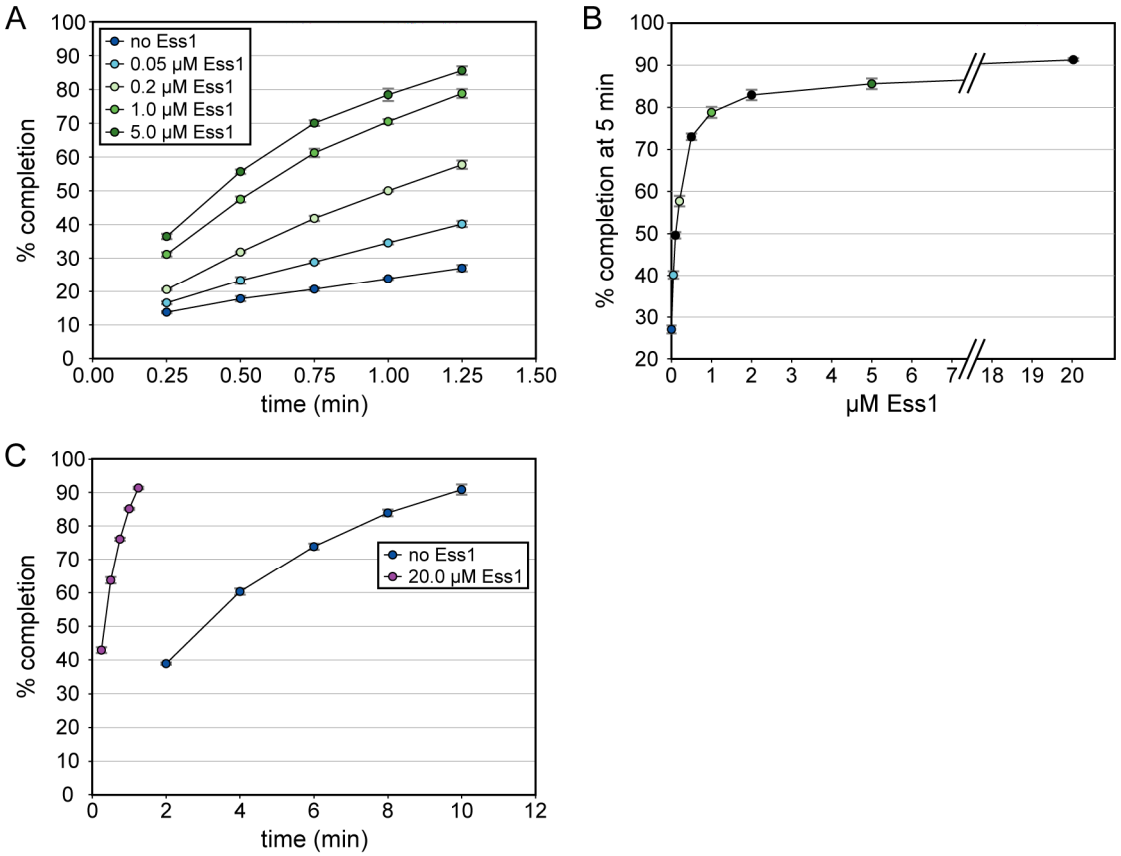

FIGURE S3. **The reaction timescale affects stimulation of Ssu72 activity by Ess1.** The kinetics in this figure are analogous to those in Figure 4 from the main text. Reactions were performed with 20 μM Ssu72 and measured at 15 second increments. In *A-C*, each point represents the average from three independent reactions and error bars denote standard deviations. *A*, the activity of Ssu72 was monitored with various concentrations of the proline isomerase Ess1. The maximum stimulation was 3.4-fold under these conditions. These reactions effectively illustrate the 'burst phase' in the absence of catalyzed proline isomerization, which results from dephosphorylation of the initial *cis* proline substrate population. In the reaction without Ess1, the first ~14% of substrate is hydrolyzed in the first 15 seconds, followed by a slow and nearly linear rate of reaction that requires a full minute to hydrolyze the second 14% of substrate (15 seconds to 1.25 minutes). *B*, Ess1 enhancement of Ssu72 activity is saturable. The last points of the reactions in *A* are plotted versus Ess1 concentration, with black circles representing reactions omitted from *A* for clarity. *C*, pCTD dephosphorylation by Ssu72 reaches completion without Ess1. The 'no Ess1' reaction in *A* was monitored over 10 minutes, and reaches ~90% completion in 10 minutes, 8-fold slower than the reaction with 20 μM Ess1.

Experimental Procedures

Protein Expression and Purification—Both Ssu72 and Ess1 were overexpressed as N-terminal 6X His-tagged constructs in *Escherichia coli* Rosetta 2 cells (EMD Biosciences, Inc.). For Ssu72, bacterial cells were induced overnight with 0.5 mM IPTG at 25°C; for Ess1, cells were induced for 3 hours with 1.0 mM IPTG at 37°C. Proteins were purified with Ni^{2+}-NTA resin (Qiagen) and His tags were removed by thrombin digestion. A second Ni^{2+}-NTA column was used to remove uncleaved protein, followed by a size exclusion column (Superdex 200, GE Healthcare) equilibrated with 25 mM Tris-HCl, 25 mM KCl buffer at pH 8.0. NMR samples were exchanged into a similar buffer with deuterated Tris-HCl, 2 mM DTT and 7% D_2O. Samples of dSsu72 for kinetic experiments also used a similar buffer but with 10% glycerol and 2 mM DTT. Crystallography samples were stored in 25 mM HEPES, 25 mM KCl, 2 mM DTT buffer at pH 8.0. Ess1 samples were exchanged into kinetics buffer. All proteins samples used for crystallography and kinetics were flash frozen in liquid nitrogen and stored at -80°C. Contrary to a previous report (2), dSsu72 was found to be monomeric by analytical ultracentrifugation in a variety of buffer conditions. Circular dichroism experiments for Ess1 mutants were performed in a cacodylate buffer system and thermal denaturation was monitored at 222 nm.

Ssu72-pCTD Structure Determination—Data were collected at the SER-CAT facility at Argonne National Laboratory and processed with HKL2000 (3). Initial phases were calculated with Phaser (4) using the crystal structure of apo WT dSsu72 deposited by the Northeast Structural Genomics Consortium (pdb code 3FDF) as a search model. The final structure was obtained by iterative cycles of manual model-building with Coot (5) and refinement with Phenix using riding hydrogens (6). The crystal contains four molecules in the asymmetric unit; clear density was observed for four imidazole molecules which mediate intermolecular packing interactions, and a PEG fragment was fit into a chain of weak density at another packing interface. The excellent quality of electron density for the substrate peptide allows an unambiguous interpretation of its binding mode (Figure 2A). Analysis of the final refined structure with Molprobity (7) gave a geometry score of 1.35 (99^{th} percentile) and a clash score of 4.27 (99^{th} percentile). Full statistics for the dSsu72-pCTD structure determination are shown in Table 1. In Figure 1, the Lpt1 sequence is aligned with Ssu72 based on its topological similarity using the DALI server (8).

CTD Peptide Preparation and Characterization—Lyophilized pCTD peptide with the sequence Ac-PTpSPSYS-NH_2 was purchased at >98% purity (CPC Scientific, Inc.). Stocks were made at neutral pH with concentrations of about 100 mM by resuspension in distilled water. Initial estimates of concentration were calculated using the Abs_{280nm}. Final concentrations were obtained by measuring the peptide's phosphate content using the base hydrolysis method and the Malachite green assay with 25 µL sample volumes (9). Standard curves were constructed from 10 points measured in triplicate; linear fits to these points were excellent with R^2 values above 0.98. To measure proline isomer populations, a natural abundance ^{13}C-HSQC experiment was collected overnight with a 10 mM peptide sample in 25 mM Na_xPO_4, 50 mM KCl, 100% D_2O buffer at pH 6.5. Proline resonances were assigned by collecting the same experiment with a shorter, single-proline peptide (TpSPSY).

Kinetics with Full-Length pCTD Substrate—Non-phosphorylated GST-yCTD-His fusion protein was overexpressed in *Escherichia coli*, purified with glutathione and Ni^{2+}-NTA resin, and dialyzed into kinase buffer (25 mM HEPES pH 7.6, 10 mM $MgCl_2$) at 4°C. Substrate was hyperphosphorylated using the CTDK-1 kinase as described previously (10), and purified over a second gluthione column. The activity of Ssu72 was monitored at room temperature with reactions containing ~4 µg of hyperphosphorylated GST-yCTD-His substrate in dephosphorylation reaction buffer (50 mM Tris-HCl pH 6.5, 10 mM NaCl, 10 mM $MgCl_2$, 0.5 mM DTT and 0.1 mM EDTA). For assays with catalyzed proline isomerization, 100 µM Ess1 was preincubated with the reaction mixture for ~20 minutes. Reactions were initiated by the addition of 100 µM dSsu72, and 25 µL aliquots were removed at the specified time points and quenched with SDS loading buffer. Aliquots were resolved on SDS-PAGE gels, and proteins were then transferred to nitrocellulose membranes for Western blot analysis. Primary antibodies were rat monoclonal anti-S5P (3E8) from D. Eick (11) and rabbit polyclonal

(affinity-purified) anti-S2P (S2) from Bethyl Laboratories, Inc. Infrared dye-labeled secondary antibodies (LI-COR Biosciences) were used to detect and quantify S5P and S2P levels with the Odyssey imaging system (LI-COR Biosciences). The plots in Figure 4F represent averages from three independent reactions, with error bars denoting standard deviations.

Supplemental References

1. Gustafson, C. L., Stauffacher, C. V., Hallenga, K., and Van Etten, R. L. (2005) *Protein Sci* **14**, 2515-2525
2. Meinhart, A., Silberzahn, T., and Cramer, P. (2003) *J Biol Chem* **278**, 15917-15921
3. Otwinowski, Z., and Minor, W. (1997) *Method Enzymol* **276**, 307-326
4. McCoy, A. J., Grosse-Kunstleve, R. W., Adams, P. D., Winn, M. D., Storoni, L. C., and Read, R. J. (2007) *J Appl Crystallogr* **40**, 658-674
5. Emsley, P., and Cowtan, K. (2004) *Acta Crystallogr D Biol Crystallogr* **60**, 2126-2132
6. Adams, P. D., Afonine, P. V., Bunkoczi, G., Chen, V. B., Davis, I. W., Echols, N., Headd, J. J., Hung, L. W., Kapral, G. J., Grosse-Kunstleve, R. W., McCoy, A. J., Moriarty, N. W., Oeffner, R., Read, R. J., Richardson, D. C., Richardson, J. S., Terwilliger, T. C., and Zwart, P. H. (2010) *Acta Crystallogr D Biol Crystallogr* **66**, 213-221
7. Davis, I. W., Leaver-Fay, A., Chen, V. B., Block, J. N., Kapral, G. J., Wang, X., Murray, L. W., Arendall, W. B., 3rd, Snoeyink, J., Richardson, J. S., and Richardson, D. C. (2007) *Nucleic Acids Res* **35**, W375-383
8. Hasegawa, H., and Holm, L. (2009) *Curr Opin Struct Biol* **19**, 341-348
9. Ekman, P., and Jager, O. (1993) *Anal Biochem* **214**, 138-141
10. Phatnani, H. P., Jones, J. C., and Greenleaf, A. L. (2004) *Biochemistry* **43**, 15702-15719
11. Chapman, R. D., Heidemann, M., Albert, T. K., Mailhammer, R., Flatley, A., Meisterernst, M., Kremmer, E., and Eick, D. (2007) *Science* **318**, 1780-1782